

# 3D tracking of transient peri-infarct depolarizations in ischemic rat brain by fast ADC mapping

Victor E. Yushmanov<sup>1</sup>, Alexander Kharlamov<sup>1</sup>, Stephen R. Yutzey<sup>2</sup>, Prahlad G. Menon<sup>1,3</sup>, Paul A. Schornack<sup>2</sup>, Erik C. Wiener<sup>2</sup>, Fernando E. Boada<sup>2</sup>, and Stephen C. Jones<sup>2,4</sup>

<sup>1</sup>Department of Anesthesiology, Allegheny-Singer Research Institute, Pittsburgh, PA, United States, <sup>2</sup>Department of Radiology, University of Pittsburgh, Pittsburgh, PA, United States, <sup>3</sup>Department of Bioengineering, Carnegie-Mellon University, Pittsburgh, PA, United States, <sup>4</sup>Departments of Anesthesiology and Neurology, Allegheny-Singer Research Institute, Pittsburgh, PA, United States

## INTRODUCTION

Peri-infarct depolarizations (PIDs) in the brain have been acknowledged as a major pathogenic factor in both early and late experimental ischemic stroke (1,2). Although PIDs have been observed in human stroke and shown to contribute to the expansion of brain infarcts, their consideration is not a part of clinical practice, which makes them an important translational research and clinical target. Despite the strong evidence that  $K^+$  is a primary driving force of PIDs, correlating the two quantitatively has been problematic because available experimental techniques,  $K^+$  microelectrodes and atomic spectroscopy (for  $K^+$ ) and laser-speckle flowmetry through a cranial window (for PID), are not suitable to follow slowly moving PID waves propagating in 3D. MRI studies using fast ADC for PIDs in rats have had limitations that include only partial coverage of the full extent of PID travel (3), limits of observation time (4-6), and ischemia models that might not be optimal for cortical PID generation (6). Here, these shortcomings were addressed with the goal of improving stroke outcome by relating PIDs to high  $[K^+]$ , and potentially creating new PID-suppressing techniques. We developed and refined 3D PID tracking protocols suitable for use in combination with innovative K/Rb substitution MRI (7) and histochemical  $K^+$  imaging, and tested the hypothesis that PID speed is variable.

## METHODS

Permanent focal cerebral ischemia was produced in 5 male Sprague-Dawley rats (500  $\pm$  100 g) by middle cerebral artery transection and bilateral common carotid artery occlusion (8) under isoflurane (in 30%  $O_2$ , 70%  $N_2O$ ) anesthesia. Images were obtained on a 7 T Bruker ClinScan using a rat head transmit/receive coil with a recirculating water bed and fittings for anesthesia gas supply. A standard diffusion-prepared twice-refocused spin echo EPI pulse sequence (TR/TE/ $\alpha$ =2500ms/43ms/90°, 64×64 matrix, 37×0.5 mm slices, 5/8 partial Fourier, FOV 32 mm, 0.5 mm<sup>3</sup> isotropic resolution) was modified to repeatedly collect control and diffusion-weighted images in 3 orthogonal directions ( $b$ -factors of 0 and 1000 s/mm<sup>2</sup>, respectively) for 3-4 h after occlusion. For anatomic reference, multislice  $T_2$ -weighted brain images were obtained. Trace ADC maps were reconstructed and all images were co-registered and analyzed using in-house developed MATLAB codes and AMIDE (9) software. For quantitative analysis of ADC changes limited to the brain only, an anatomic 3D brain mask was rendered based on a  $T_2$ -weighted image after skull-stripping. The ischemic region was defined as  $ADC < 570 \mu m^2/s$ . Difference images allowed us to track transient changes in ADC by plotting either their center of mass or their front edge in 3D. Contrary to commonly performed assessment of mean propagation speed, the speed and direction of each individual PID segment were analyzed. The infarct size and location were verified post mortem by surface reflectivity, MAP2 and  $K^+$  histological staining.

## RESULTS

In each of 5 animals, several PIDs were observed. In one of the animals, 8 PIDs were observed over 80 min of fast ADC MRI scanning with a periodicity of 10 $\pm$ 1 min (mean $\pm$ sem). Six of these PIDs were associated with spontaneous systemic blood pressure decreases (122 $\pm$ 3 mmHg before PID vs. 98 $\pm$ 4 mmHg during PID, mean $\pm$ sem, n=6, p<0.05). The PIDs were visualized as waves of ADC depression (Fig. 1), separated from the central ischemic core (area of permanently low ADC), and tracked by plotting the trajectories of either their centers of mass (Fig. 2) or of their front edge (Fig. 3). Six out of 8 PIDs originated in the dorso-caudal area of ischemic hemisphere and moved in the ventro-rostral direction (Fig. 3), and 2 had the reverse path, ventro-rostral towards the dorso-caudal area. The coefficient of variation of segment speed within and between PIDs was 50.5% vs. 16.1%.

## DISCUSSION AND CONCLUSIONS

The results represent significant advances in monitoring PIDs: a) 3D tracking, segment by segment, throughout the whole brain, including beyond the usual position of a cranial window, and b) demonstration of large between-segment variations in PID speed and of the possibility of PID origination in the subcortical areas of the brain. When combining PID tracking techniques with quantitative  $K^+$  methods (7), we expect to correlate PID propagation with  $K^+$  efflux from the brain. The overall impact will be a significant advance in the basic understanding of stroke mechanism in general, as well as a potential of developing novel techniques to minimize PID-mediated infarct expansion.

**ACKNOWLEDGMENTS:** Tiejun Zhao (Siemens Medical Solutions USA, Pittsburgh, PA) for his pulse sequence expertise; NIH grants NS30839 and NS66292.

## REFERENCES

1. Dreier JP. *Nat. Med.* 2011; **17**: 439-447.
2. Lauritzen M et al. *J. Cereb. Blood Flow Metab.* 2011; **31**: 17-35.
3. Kastrup A et al. *J. Cereb. Blood Flow Metab.* 2000; **20**: 1636-1647.
4. Gyngell ML et al. *Magn. Reson. Med.* 1994; **31**: 337-341.
5. Hasegawa Yet al. *J. Cereb. Blood Flow Metab.* 1995; **15**: 179-187.
6. Takano K et al. *Ann. Neurol.* 1996; **39**: 308-318.
7. Yushmanov VE et al. *NMR Biomed.* 2011; **24**: 778-783.
8. Jones SC et al. *Stroke* 2006; **37**:883-888.
9. Loening AM, Gambhir SS. *Mol. Imaging* 2003; **2**:131-137.
10. Paxinos G, Watson C. *The rat brain in stereotaxic coordinates*. New York: Academic Press, 1997.

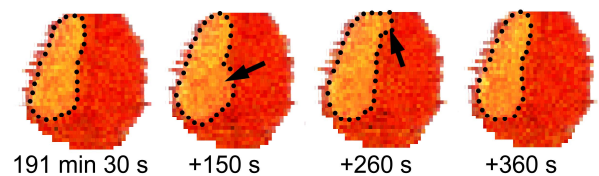


Fig. 1. Horizontal projections (i.e., sums of voxel intensities) of a 3D brain ADC map featuring an ischemic lesion (in yellow, outlined). Left: at 191 min 30 s after occlusion. To the right: PID origination at the edge of the ischemic lesion, its caudal-rostral propagation (arrows) and eventual disappearance of a PID.

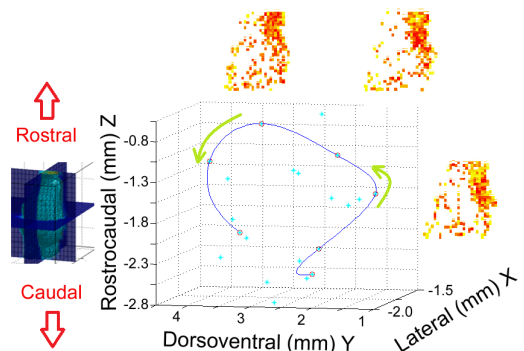


Fig. 2. A B-spline-smoothed path of the center of mass of the traveling depolarization wave (+150 to +350 s, Fig. 1). Sagittal images illustrate the propagation of a low-ADC ischemic lesion (in orange) along the path.

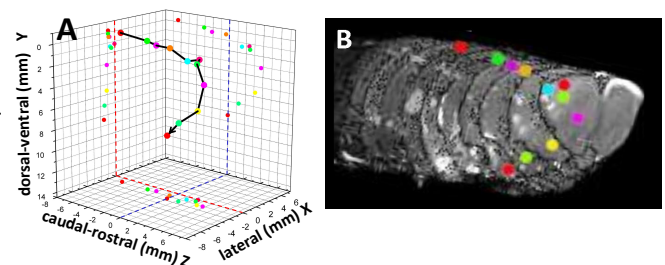


Fig. 3. A: A trajectory of the propagating front edge of the low ADC wave during the PID event in ischemic brain. Arrow indicates the propagation direction. The PID speed is variable: the time gap between the color-coded dots is 10 s. The projections of the PID trajectory in Paxinos & Watson (10) coordinates are shown. PID propagation started from the dorsal part of the brain surface (-6.2 mm from bregma) and moved rostrally, then 'dived' around the frontal pole, ending up rostral to the Circle of Willis. Red lines indicate the mid-sagittal plane, blue lines indicate the bregma level. B: PID propagation demonstrated by the sequential PID positions shown by the color-coded dots superimposed over the  $T_2$ -weighted brain image for anatomic reference.